Tellus (2002), 54B, 61–73
Printed in UK. All rights reserved

TELLUS
ISSN 0280–6509

Maritime/continental microphysical contrasts in stratus

By SEONG SOO YUM* and JAMES G. HUDSON†, *Division of Atmospheric Sciences, Desert Research Institute, 2215 Raggio Parkway, Reno, Nevada 89512-1095, USA*

(Manuscript received 23 November 2000; in final form 25 September 2001)

ABSTRACT

More than 15 h of in situ cloud measurements in Atlantic and Pacific stratus showed cloud droplet concentrations to be correlated with cloud condensation nuclei (CCN) concentrations measured just below cloud. Predictions of droplet concentrations based on complete CCN spectra and measured updraft velocities were better correlated with measured cloud droplet concentrations. This was especially significant for near-adiabatic parcels because these results represent a good level of closure between CCN and cloud microphysics. Over the Atlantic there was a clear dichotomy between maritime and continental cloud microphysics that was related to CCN concentrations: smaller and more numerous droplets in continental clouds with higher CCN concentrations. However, there seemed to be undercounting of continental cloud droplets because many were smaller than the 2 μm diameter threshold of the droplet spectrometer. When averaged over all altitudes, the drizzle (diameter >50 μm) liquid water content was a factor of 2 greater in the maritime clouds. However, as in previously reported small cumuli, drizzle was also a function of cloud depth. Therefore when only thin clouds (depth less than 45 mb) were considered, the maritime clouds had an order of magnitude more drizzle than continental clouds. Drizzle liquid water content was also found to depend on the mean diameter of 2–50 μm diameter cloud droplets. In the thin clouds there was a definite 15 μm mean cloud droplet diameter threshold for the onset of drizzle that was often exceeded in the maritime clouds but almost never exceeded in the continental clouds. There were also higher concentrations of 20–50 μm diameter droplets in the maritime clouds that were commensurate with the maritime/continental drizzle (50–620 μm diameter) contrast. Furthermore, when cloud parcels with equal amounts of cloud droplet liquid water were compared, there was considerably more drizzle in the maritime clouds, especially for larger amounts of cloud water in the thin clouds. All of these maritime/continental contrasts found in thin stratus clouds are very similar to previously reported maritime/continental contrasts in small cumulus clouds. These results support the second indirect aerosol effect (pluvial inhibition) for stratus clouds.

1. Introduction

One of the most important influences on cloud microphysics is the cloud condensation nuclei (CCN) distribution in the lower atmosphere (e.g., Hudson, 1993). Despite other influences on cloud droplet concentrations (N_c) (e.g., Twohy and Hudson, 1995), there was a close relationship between measured CCN concentrations (N_{CCN}) and N_c for cumuli (Twomey and Warner, 1967), for stratus clouds over the Southern Ocean (Yum et al., 1998), for eastern Atlantic stratus (Snider and Brenguier, 2000), and small cumulus clouds over eastern Florida (Hudson and Yum, 2001, HY01 hereafter). These results support the first Twomey effect (Twomey, 1977) or the first indirect aerosol effect (Charlson et al., 1992): greater cloud albedo due to more numerous droplets. The largest

* Present affiliation: Department of Atmospheric Sciences, Yonsei University, Seoul 120-749, Korea.
e-mail: ssyum@atmos.yonsei.ac.kr
† Corresponding author.
e-mail: hudson@dri.edu

maritime/continental contrast was, however, in drizzle (HY01). Greater drizzle in maritime clouds is consistent with precipitation suppression in convective tropical clouds infected by heavy smoke (Rosenfeld, 1999) and in clouds formed over urban pollution sources (Rosenfeld, 2000). These studies then support the second Twomey effect (Hudson, 1993), pluvial inhibition (e.g., Albrecht, 1989), which Rotstayn (1999) showed to be comparable to the first Twomey effect.

Efforts to understand relationships between CCN and cloud microphysics are advanced in this study of summertime marine stratus environments over eastern sides of mid-latitude Northern Hemisphere oceans. These results also support the basis of both the first and second indirect aerosol effects.

2. Experiment

Data used in this study came from measurements in two aircraft field projects, FIRE [First ISCCP (International Satellite Cloud Climatology Project) Regional Experiment] (Albrecht et al., 1988) off the west coast of mid-latitude North America and ASTEX (Atlantic Stratocumulus Transition Experiment) (Albrecht et al., 1995) over the mid-latitude eastern North Atlantic. On five of the FIRE flights, both CCN and cloud microphysics were measured. All 17 ASTEX flights measured CCN and cloud microphysics, but one flight was excluded for lack of clouds whereas data from two distinct air masses in one flight were considered separately (Hudson and Li, 1995). Air mass changes also occurred during four other ASTEX flights, but for those flights only data from the dominant air mass were used in this analysis. Overall there are then 6 continental and 11 maritime flights during ASTEX, whereas all five FIRE flights were generally considered maritime. A detailed description of CCN and condensation nuclei (CN) measurements and air mass designations during FIRE and ASTEX were presented by Hudson and Xie (1999).

A standard Particle Measuring Systems (PMS) Forward Scattering Spectrometer Probe (FSSP-100) was used to measure cloud droplets between approximately 2 and 50 μm diameter. Drizzle drops (50–620 μm diameter) were measured by a PMS 260X probe (as in our previous publications 260X channels below 50 μm were discarded). Operation of these PMS probes has been discussed by Knollenberg (1981), Baumgardner (1983), and Baumgardner and Spowart (1990). An N_c threshold of 1 cm^{-3} was used to define clouds. Since all cloud data are 1 s averages, this means that at average aircraft speed of 100 m s^{-1} they are averages over 100 m.

3. Results

3.1. Air mass differences

Table 1 shows the contrasts between maritime and continental air masses and similarities between the two maritime projects (FIRE and ASTEX maritime). Hudson and Xie (1999) designated continental or maritime according to air trajectories. ASTEX continental shows both highest CN and CCN concentrations (N_{CN} and N_{CCN}; rows 2 and 3, Table 1) and highest cloud droplet concentrations (N_c) (rows 6 and 7, Table 1).

Table 1. *Project averages of boundary layer CN and CCN concentrations, and cloud microphysical parameters obtained by averaging flight averages for each project or air mass*

	Parameter	FIRE maritime	ASTEX maritime	ASTEX continental
1	Total data (s)	18 120	35 869	13 221
2	N_{CN} (cm^{-3})	251	393	1377
3	N_{CCN}(0.6%)	110	163	1023
4	L_c (g^{-3})	0.106	0.126	0.098
5	L_c/L_a	0.108	0.131	0.114
6	N_c(av) (cm^{-3})	41	86	183
7	N_{binmax} (cm^{-3})	101	204	438
8	MD (μm)	15.0	11.9	8.0
9	D_v (μm)	17.0	13.9	9.8
10	D_e (μm)	19.6	16.3	12.1
11	$K = D_v^3/D_e^3$	0.68	0.63	0.55
12	L_d (g m^{-3})	0.048	0.038	0.021

Here N_{CN} is the CN concentration, N_{CCN} is the CCN concentration at 0.6% supersaturation, L_c is the cloud droplet (2–50 μm diameter) liquid water content, L_a is the adiabatic L_c, N_c(av) is the average cloud droplet concentration, N_{binmax} is an estimate of adiabatic N_c, MD is the mean cloud droplet diameter, D_v is the cloud droplet mean volume diameter, D_e is the cloud droplet mean effective diameter, and L_d is the drizzle (50–620 μm diameter) liquid water content. Rows 4–11 refer only to droplets measured by the FSSP (~2–50 μm diameter).

However, the factor of six greater continental N_{CCN} compared to maritime is three times more than the factor of two greater N_c of continental over maritime ASTEX. The smaller continental/maritime N_c ratio than N_{CCN} ratio is expected due to elevated competition in the continental clouds. Competition among CCN for condensed water can reduce cloud supersaturation (S) (i.e., Twomey, 1959). This means that continental N_c is more closely related to N_{CCN} at a lower S than maritime. Since N_{CCN} at lower S are lower, this means that continental N_c is not as much higher than maritime N_c compared to how much higher continental N_{CCN} is than maritime N_{CCN} at the same S.

The smaller sizes of the continental cloud droplets (rows 8–10, Table 1) suggest the possibility that more of the continental droplets may be below the FSSP threshold size of 2 μm. In Fig. 1 the higher relative concentrations in the smallest FSSP size channels for continental clouds compared to maritime clouds confirms that actual continental cloud droplet concentrations are underestimated relative to maritime clouds. The effect of this is to also reduce the continental/maritime N_c ratio relative to the N_{CCN} ratio. Therefore, there are two independent explanations for the smaller continental/maritime N_c ratios compared to the continental/maritime N_{CCN} ratios: greater competition and undercounting of N_c in continental clouds.

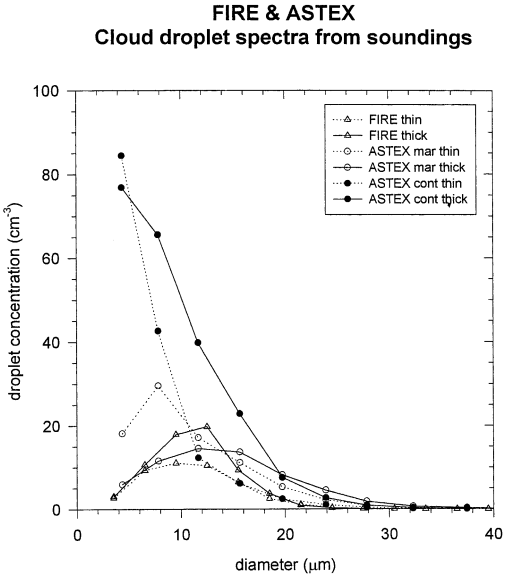

Fig. 1. Average cloud droplet spectra per bin from the FSSP-100 for sounding data. Thin and thick cloud depths (cd) are defined at 45 mb.

FIRE shows both the lowest N_{CCN} (row 3, Table 1) and N_c (rows 6 and 7, Table 1). However, contrary to the ASTEX continental/maritime comparison, the ratio of the two maritime (ASTEX/FIRE) N_c values is greater than the N_{CCN} ratio; i.e., the factor of 2 greater ASTEX N_c than FIRE N_c is larger than the 50% higher N_{CCN} of ASTEX over FIRE N_{CCN}. Relative ratios of N_c and N_{CCN} for the two maritime air masses that are opposite to those of the two ASTEX air masses therefore cannot be attributed to either of the explanations in the last paragraph. Moreover, neither explanation applies because there is not enough competition in either maritime air mass to cause significant reductions of S, and Fig. 1 shows that there was minimal undercounting of cloud droplets in the maritime air masses. The larger N_c ratio than N_{CCN} ratio could be attributed to more entrainment, more drizzle, or lower updrafts (W) in FIRE than ASTEX maritime. Entrainment can be represented by L_c/L_a (row 5, Table 1; L_c is the liquid water content of 2–50 μm diameter cloud droplets and L_a is adiabatic L_c; L_a was calculated for each data point based on distance from cloud base and cloud base temperature); the smaller ratio for FIRE indicates more entrainment. Drizzle is a result and cause of droplet coalescence, which reduces N_c. The last row of Table 1 shows greater drizzle in FIRE. Greater cloud depth and more cumuliform structures in ASTEX suggest higher W. ASTEX, after all, was an investigation of the transition to trade cumuli, which generally have higher W than stratus. Therefore, all three of these factors, entrainment, drizzle and W, increase the N_c difference relative to the N_{CCN} difference between ASTEX maritime and FIRE.

The 49% larger mean diameter (MD) (row 8, Table 1) of droplets in ASTEX maritime compared to ASTEX continental is commensurate with the fact that maritime N_c(av) (row 6, Table 1) was 47% of continental, and maritime L_c (row 4, Table 1) was 29% higher than continental L_c, because droplet size is proportional to the cube root of L_c/N_c; the cube root of 1.29/0.47 is 1.40. This agreement is especially good considering that Fig. 1 suggests that continental N_c(av) and thus

L_c were underestimated and MD was overestimated. The 26% greater average MD of FIRE over ASTEX maritime is commensurate with the fact that FIRE N_c(av) was 48% of ASTEX maritime N_c(av), while FIRE L_c was 84% of ASTEX maritime L_c; the cube root of 0.84/0.48 is 1.21. As should be expected, the observed cloud droplet volume mean diameter (D_v; row 9, Table 1) ratios of 1.42 for ASTEX maritime to continental and 1.22 for FIRE over ASTEX maritime, are much closer to droplet size ratios calculated from average N_c and L_c, namely 1.40 and 1.21, respectively. The lower N_{CCN} and N_c of FIRE may have contributed to the 25% greater drizzle (row 12, Table 1) in FIRE compared to ASTEX maritime, which has a factor of 2 greater drizzle than ASTEX continental that is inversely proportional to the N_c ratio.

3.2. *Comparisons of CCN with cloud droplet concentrations*

Rows 1–5, Table 2 show linear regressions and average ratios of below-cloud N_{CCN} averages for each flight with averages of N_c [N_c(av)] for each flight. The average ratios of the flight average N_{CCN} to N_c(av) (column 6) are more than 1.0 except for N_{CCN} at S below 0.1%. This implies an effective S (S_{eff}) of $<0.1\%$ (i.e., Hudson, 1984). However, the correlation coefficients (γ) (column 5) for N_{CCN} versus N_c(av) at these lower S values are smaller than for N_{CCN} at higher S. There is considerable divergence in the ratios for the three projects/air masses (columns 7–9). The values of S of the row with the N_{CCN}/N_c ratio closest to 1.0 provides an estimate of S_{eff}. This suggests the lowest S_{eff} for ASTEX continental and the highest S_{eff} for ASTEX maritime. This is consistent with arguments in the last section that competition reduces S in continental while lower W and/or more entrainment and drizzle in FIRE makes relatively lower droplet concentrations and thus lower S_{eff} than ASTEX maritime.

Yum et al. (1998) recounted the pitfalls of comparing average cloud droplet concentrations [N_c(av)] with N_{CCN} because N_c(av) can be reduced by dilution and evaporation of entrainment, cloud edge artifacts, and droplet coalescence. All of these

Table 2. *Linear regressions of CCN concentrations (N_{CCN}) at various supersaturations (S) versus three representations of cloud droplet concentrations (N_c) [average, binmax, and near-adiabatic parcels] and average ratios of concentrations combined and separate*

Cloud droplet concentration (N_c)	Aerosol	b	a	γ	Ratio N_{CCN}/N_c			
					All	FIRE mar.	ASTEX mar.	ASTEX cont.
N_c(av)	N_{CCN}(0.6%)	−160	5.32	0.78	3.31	2.50	2.26	5.90
	N_{CCN}(0.4%)	−149	4.65	0.77	2.73	2.17	1.63	5.22
	N_{CCN}(0.2%)	−66	2.61	0.72	1.71	1.56	0.92	3.29
	N_{CCN}(0.1%)	−32	1.51	0.66	1.05	1.03	0.53	2.04
	N_{CCN}(0.02%)	−9	0.47	0.55	0.35	0.41	0.12	0.71
N_{binmax}	N_{CCN}(0.6%)	−247	2.59	0.86	1.28	0.98	0.79	2.43
	N_{CCN}(0.4%)	−222	2.25	0.85	1.07	0.85	0.59	2.15
	N_{CCN}(0.2%)	−108	1.27	0.79	0.68	0.61	0.34	1.36
	N_{CCN}(0.1%)	−57	0.74	0.73	0.42	0.40	0.20	0.84
	N_{CCN}(0.02%)	−16	0.23	0.60	0.14	0.16	0.04	0.29
N_c(parcels)	N_{CCN}(0.6%)	−8	1.12	0.72	1.15	1.69	0.72	1.63
	N_{CCN}(0.4%)	1	0.85	0.67	0.96	1.48	0.57	1.27
	N_{CCN}(0.2%)	46	0.15	0.29	0.67	1.10	0.37	0.35
	N_{CCN}(0.1%)	43	−0.04	0.11	0.43	0.96	0.21	0.10
	N_{CCN}(0.02%)	18	−0.06	0.31	0.14	0.32	0.02	0.02

Here b is the intercept of the linear regression, a the slope of the linear regression, γ the correlation coefficient. The total number of data points is 22 for av and binmax (this is the number of flights), whereas the number of near-adiabatic parcels is 27 (11 for FIRE, 15 and 1 for ASTEX maritime and continental, respectively).

factors reduce N_c from the N_c that originally formed on CCN at cloud base. Since these processes are variable, they can disguise the influence of N_{CCN} on N_c. Therefore, a more useful N_c to compare with N_{CCN} would be N_c in adiabatic cloud parcels (N_a), which have not been affected by entrainment, cloud edges or coalescence.

Yum et al. (1998) estimated N_a by sorting droplet concentration data into bins and choosing the highest bin with at least 3 data points; this is N_{binmax}, row 7, Table 1 and rows 6–10, Table 2. Since N_{binmax} is higher than N_c(av), the N_{CCN} to N_{binmax} ratios (columns 6–9, rows 6–10, Table 2) are lower than N_{CCN}/N_c(av) (rows 1–5). N_{binmax} thus implies higher S_{eff} than N_c(av). The N_{CCN}/N_{binmax} ratios closest to 1.0 show this and the same S_{eff} hierarchy: lowest S_{eff} for continental and highest S_{eff} for ASTEX maritime. The correlation coefficients (γ) for N_{CCN} with N_{binmax} (column 5) are higher than those for N_c(av) and, as with N_c(av), γ are greater for N_{CCN} at higher S. Similar to the comparisons and discussions of Table 1 in Section 3.1, the ratios of N_{CCN} to both N_c(av) and N_{binmax} are highest for continental and lowest for ASTEX maritime (columns 7–9, rows 1–10, Table 2).

Yum et al. (1998) also used near-adiabatic cloud parcels to estimate N_a. These were identified by high constant cloud droplet concentrations (N_c) and minimal drizzle. Rows 11–15, Table 2 present linear regressions and ratios of nearby cloud base N_{CCN} to average N_c in 27 near-adiabatic cloud parcels. High correlation coefficients (γ) are found only for N_{CCN} above 0.3% S. Although these γ values for high S are slightly smaller than those for average and binmax, the intercepts (b) are closer to zero, and the slopes (a) and ratios (column 6) are closer to 1.0. For ASTEX maritime the parcel ratios (column 8) are nearly identical to corresponding binmax ratios, but for FIRE these ratios (column 7) are higher than corresponding rows for binmax. Therefore, for ASTEX maritime the estimates of S_{eff} are the same for binmax and parcel. Both binmax and parcel estimates of S_{eff} are higher for ASTEX maritime than for FIRE but the S_{eff} difference is greater when based on parcels. Since these adiabatic parcels should be less subject to entrainment and coalescence this gives a stronger indication that W was indeed higher in ASTEX and that higher W was the cause of the higher S_{eff} of ASTEX maritime over FIRE. Parcel ratios for continental (column 9) are much lower than they are for binmax. This last parcel column, however, is based on just a single continental adiabatic parcel, which had a droplet spectrum that suggested minimal undercounting compared to most continental spectra. The fact that 26 of the 27 near-adiabatic parcels were maritime is probably one reason for the lower parcel γ than the γ values for average and binmax, which have a mix of 6 continental and 16 maritime flights. Greater concentration variations tend to produce better correlations. Therefore, on the whole, N_{CCN} probably predicts N_c in adiabatic parcels better than it does N_c(av) or N_{binmax}. However, the closer similarities of the binmax and parcel N_{CCN}/N_c ratios, at least compared to ratios with N_c(av), especially FIRE, suggest that N_{binmax} and N_c(parcel) may be reasonable approximations of adiabatic cloud droplet concentrations (N_a).

The linear regressions and ratios for all of the separate air mass/project $N_{CCN}(0.6\%)/N_c$ relationships are displayed in Table 3. N_{CCN} for this highest $S(0.6\%)$ of which Hudson and Xie (1999) were confident had the highest correlation coefficients (γ) for all air masses/projects. FIRE shows good correlations for all three N_c (rows 1, 5 and 9) and ASTEX maritime has good correlations for binmax and parcels (rows 6 and 10). ASTEX continental shows no correlation (rows 3 and 7; only one continental data point prevented a parcel regression). The bad continental correlations may be due to: (1) cloud supersaturation (S) variations due to competition, which, as pointed out earlier, changes the value of S for which N_{CCN} is most closely related to N_c, which then confounds correlations between N_c and N_{CCN} at a specific S; or (2) undercounting of cloud droplets (e.g., Fig. 1), which probably varied among the flights. As in Table 2, binmax always shows the highest γ of the three representations of N_c, except for ASTEX-combination data. Also, like Table 2, parcels have the smallest intercepts (b) and slopes (a) that are closest to 1.0. For all three droplet representations the combined ASTEX data show much better correlation coefficients than the separated ASTEX data.

3.3. *Predictions*

Cloud droplet concentrations can be predicted (N_p) by applying the adiabatic condensation model

Table 3. *As Table 2 except only $N_{CCN}(0.6\%)$ is correlated with cloud droplet concentrations (N_c) for data divided according to projects or air masses*

N_c	Project/air mass	n	b	a	γ	Ratio N_{CCN}/N_c
N_c(av)	FIRE-mar.	5	−110	5.30	0.78	2.50
	ASTEX-mar.	11	76	1.01	0.37	2.26
	ASTEX-cont.	6	958	0.36	0.05	5.90
	ASTEX-both	17	−213	5.64	0.74	3.54
N_{binmax}	FIRE-mar.	5	−137	2.44	0.97	0.98
	ASTEX-mar.	11	−103	1.30	0.78	0.79
	ASTEX-cont.	6	669	0.81	0.27	2.43
	ASTEX-both	17	−360	2.88	0.85	1.37
N_c(parcels)	FIRE-mar.	11	−9	1.88	0.63	1.69
	ASTEX-mar.	15	−18	0.85	0.61	0.72
	ASTEX-both	16	−167	1.93	0.93	0.78

n is the number of data points (number of flights or number of parcels).

of Robinson (1984) to the measured complete CCN spectra and updraft velocities (W). This model produced better results than the Twomey (1959) equation (Yum et al., 1998). N_p for the first two rows of Table 4 were computed based on average cloud base CCN spectra and average W measured within the clouds of each flight. N_p for the last row of Table 4 was computed from CCN spectra beneath each cloud parcel and W measured within each cloud parcel.

In spite of various normalization schemes, the prevalence of negative W in ASTEX clouds (both averages and parcels) suggested W measurement inaccuracies. Moreover, several reasons were given in Sections 3.1 and 3.2 to suggest higher W for ASTEX than FIRE. This is further substantiated by the fact that for a majority of the comparisons in ASTEX maritime (especially parcels) N_c exceeded N_{CCN} at the highest S of 1%. This meant that only the lower bounds of effective supersaturations (S_{eff}) could be estimated, and it prevented accurate N_p. Although continental N_{CCN} always exceeded N_c, these underestimations of continental cloud droplet concentrations undermined N_p–N_c relationships. Limitations of all three necessary measurements (N_{CCN}, N_c and W) in ASTEX, therefore, restricted this analysis to FIRE, where all three measurements appeared to be adequate to the task.

Table 4. *As Table 3 except that predictions of N_c (N_p) are compared with cloud droplet concentrations for FIRE*

Droplet concentration	n	b	a	γ	Ratio N_p/N_c	sl (%)
N_c(av)	5	−38	2.88	0.65	1.90	88
N_{binmax}	5	−84	1.63	0.99	0.74	99.95
N_c(parcels)	11	1	1.15	0.62	1.14	97.7

The last column is the significance level.

Table 4 then presents predicted (N_p) versus measured N_c only for FIRE. The maximum possible condensation coefficient (1.0) was used for the model predictions in Table 4. When 0.036 was used for the condensation coefficient, N_p was 12–14% higher. As with Tables 2 and 3, binmax shows the highest and parcel shows the lowest correlation coefficient (γ), and parcel shows the lowest intercept (b) and slope (a), which are, respectively, closest to zero and 1.0. The ratios for all three N_c are lower in Table 4 than the corresponding FIRE ratios in Table 3. Although both tables show the FIRE parcel ratios intermediate to the other two ratios, Table 4 is the only one with the parcel ratio closest to 1.0. Moreover, compared to the corresponding rows of Table 3, all of the intercepts are closer to zero and all of the slopes and ratios, except binmax, are closer to 1.0. This means that in spite of slightly lower γ for N_c(av) and N_c(parcel), N_p (Table 4) are better predictors of N_c than N_{CCN} (Tables 2 or 3). This is probably because the model accounts for different supersaturations (S) due to different CCN spectral shapes and varied W. Figure 2 displays

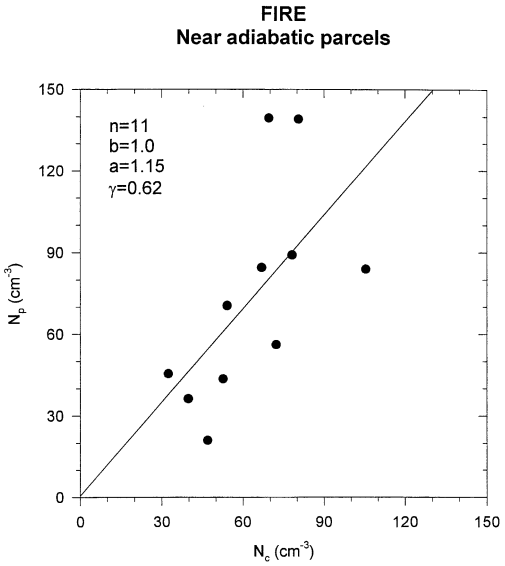

Fig. 2. Predictions of N_c (N_p) versus cloud droplet concentrations (N_c) for near-adiabatic parcels in FIRE.

the data for the FIRE parcel regression of the last row of Table 4. Apparently, since the model predictions and the use of adiabatic parcels account for most other variables, this shows a good level of CCN–cloud droplet closure. When 0.036 was used for the condensation coefficient, γ was lower and the slope and ratio were 15% higher.

3.4. *Effective supersaturations (S_{eff})*

Table 5 shows inferred median effective supersaturations (S_{eff}), which are obtained by comparing CCN spectra with cloud droplet concentrations (N_c) (e.g., Hudson, 1984). Flight averages of each are used for the first two rows. For the last row, CCN spectra just below each cloud parcel are compared with average droplet concentrations in each parcel. As expected, these median S_{eff} are consistent with the S_{eff} based on the N_{CCN}/N_c ratio that is closest to 1.0 in Table 2. S_{eff} based on N_c(av) are lower because of the reductions of N_c by entrainment and coalescence. Table 5 indicates lowest S_{eff} for continental (at least for the first 2 rows) because of competition, and highest S_{eff} for ASTEX maritime because of less entrainment, less drizzle, or higher W than FIRE, even for somewhat higher N_{CCN} than FIRE. Since binmax and especially parcel data should factor out entrainment and drizzle; this leaves W as the principal reason for the differences between the two maritime data sets. Again the higher S_{eff} for continental parcels is due to the lack of droplet undercounting for this single parcel compared to the other continental measurements. Therefore, the higher parcel S_{eff} for continental than FIRE may also substantiate the higher W of ASTEX, which then seems to be a stronger influence on cloud S than N_{CCN}. However, this lone continental parcel does not provide much assurance that higher W overcame higher N_{CCN} to make S_{eff} higher in continental than FIRE. Nevertheless, when this parcel S_{eff} is compared with the other continental S_{eff}, it gives an idea of the artificial underestimates of S_{eff} due to undercounting of continental cloud droplets. Thus the reduction of S_{eff} by high N_{CCN} is not as great as indicated by the comparisons in rows 1 and 2 of Table 5. Nonetheless, for all N_c representations, continental had lower S_{eff} than ASTEX maritime, which probably had similar W. The two S_{eff} based on predictions (N_p) for FIRE are consistent: 0.31 and 0.27% for average and parcel, respectively. These are intermediate to S_{eff} for binmax and parcel in Table 5. They, of course, exceed S_{eff} for N_c(av) because S_{eff} is underestimated because entrainment and coalescence reduce cloud droplet concentrations. These predicted S_{eff} are only slightly lower than the maximum supersaturations (S) computed by the adiabatic cloud model. This slight difference is due to discrete $N_{CCN}(S)$ bins rather than continuous $N_{CCN}(S)$ distributions, and because there is some deactivation of CCN that have critical supersaturations (S_c) just below the maximum S.

Table 5. *Median effective supersaturations (S_{eff}) in percent based on three representations of cloud droplet concentration (N_c) measurements*

Cloud droplet concentrations	FIRE mar.	ASTEX mar.	ASTEX cont.
N_c(av)	0.08	0.31	0.04
N_{binmix}	0.48	>1.00	0.17
N_c(parcels)	0.19	>1.00	0.34

3.5. *Comparisons with drizzle*

The maritime/continental difference in droplet concentrations (N_c) and sizes are commensurate

with the maritime/continental differences found in the Small Cumulus Microphysics Study (SCMS) by HY01 [e.g., a factor of 2 in N_c(av) and 50% in MD], but the maritime/continental differences in drizzle (L_d; row 12, Table 1) are only a factor of 2 [also reported for ASTEX by Hudson and Li (1995) and Hudson and Yum (1997)]. This is much less than the factor of 18 for the corresponding SCMS maritime/continental L_d difference (HY01). On the other hand the average L_d for these stratus clouds is larger than SCMS even though the stratus clouds are considerably thinner: 40 mb compared to 200 mb. The factor of 2 lower N_c for both air masses in ASTEX compared to SCMS may have enhanced drizzle in ASTEX relative to SCMS, but the longer lifetime of the stratus also enhances drizzle relative to cumuli. The average L_d in maritime stratus exceed the average (over all altitudes) for maritime cumulus by 50%, but the continental stratus exceed the continental cumuli average L_d by an order of magnitude. Figure 3, however, shows that, as in the cumulus clouds (HY01), L_d in these stratus clouds is also dependent on cloud thickness. This is illustrated differently than for the cumuli (HY01)

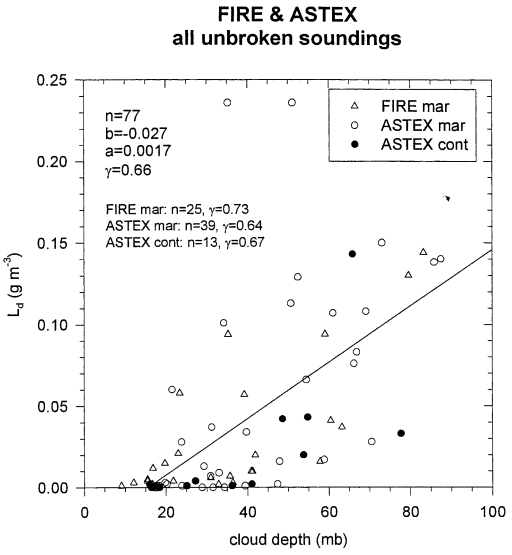

Fig. 3. Average drizzle liquid water content (L_d) (for drops 50–620 μm diameter) versus cloud depth (cd) of soundings. Also shown is the linear regression, where n is the number of data points, b is the intercept, a is the slope and γ is the correlation coefficient. n and γ for each air mass is also shown.

because the smaller vertical extent and greater lifetimes of stratus produce more vertical redistributions (i.e., fall) of L_d. Hudson and Yum (1997) showed that, contrary to observations in small cumuli (HY01), there is generally more drizzle toward the bases rather than the tops of stratus (also noted by Nicholls, 1984) in both ASTEX and FIRE. For all of these reasons it was necessary to limit cloud depth perceptions to data obtained in vertical soundings that went through both cloud base and cloud top. Average L_d for cloud soundings was found to be related to cloud thickness for both continental and maritime clouds in both projects (Fig. 3).

Since Fig. 3 shows no significant drizzle ($L_d < 0.01$ g m^{-3}) in continental clouds with depths less than 45 mb, we divided the data at cloud depth (cd) 45 mb to produce Table 6. For thin clouds the last row of Table 6 shows a factor of 13 and 17 greater maritime L_d than continental. This is comparable to the factor of 18 all-altitude average maritime/continental L_d contrast for small cumuli (HY01). Thick clouds, which have more L_d, show only a factor of 2 greater L_d for maritime over continental. Apparently even continental cloud microphysics can produce significant drizzle in thick stratus.

For all variables, Table 6 shows similar maritime/continental contrasts to those in Table 1. With the slight exception of FIRE, the droplets are, as expected, larger in the thick clouds (row 6, Table 6). There was no perceptible systematic variation of mean diameter (MD) or N_c with cd, except possibly for continental N_c, where some droplets are below the detection threshold.

Figure 4 shows a strong dependence of drizzle (L_d) on MD. As in Table 6, the maritime/continental drizzle contrast is more pronounced in the thin clouds (Fig. 4a), where there is less drizzle than the thick clouds (Fig. 4b). Drizzle was almost nonexistent in thin continental clouds, but depends very much on MD in both thin and thick maritime clouds. Figure 4a shows a sharp 15 μm MD threshold for drizzle in thin maritime clouds that was never exceeded in thin continental clouds. Figure 5 shows that the same amount of cloud droplet (2–50 μm diameter) liquid water (L_c) produces more drizzle (50–620 μm diameter) in maritime than continental clouds for both thin and thick stratus. Figures 4a and 5a for thin stratus are very similar to corresponding figures

Table 6. *Averages divided according to cloud thickness (thin <45 mb; thick >45 mb)*

	Thin			Thick		
	FIRE mar.	ASTEX mar.	ASTEX cont.	FIRE mar.	ASTEX mar.	ASTEX cont.
Total data (s)	1482	1167	440	992	2143	927
cd (mb)	27	26	25	67	66	60
N_{CN} (cm^{-3})	252	364	1439	325	241	1343
N_{CCN}(0.6%) (cm^{-3})	112	126	1032	157	131	947
N_c(av) (cm^{-3})	44	85	149	66	61	217
MD (μm)	13.7	11.4	7.6	13.4	14.3	9.4
L_c ($g\,m^{-3}$)	0.0841	0.1031	0.0614	0.1225	0.1539	0.1698
L_d ($g\,m^{-3}$)	0.0176	0.0233	0.0014	0.0770	0.0996	0.0562

These microphysical averages are the averages of the averages over all altitudes of each individual sounding in each air mass/project.

from small cumulus clouds (HY01) in terms of the maritime/continental drizzle contrasts.

ASTEX data from Fig. 1 are displayed logarithmically in Fig. 6, which shows that although continental total cloud droplet concentrations are greater, the concentrations of large cloud droplets (20–50 μm diameter) are greater in maritime clouds. Concentrations of larger droplets are also greater in the thick clouds than in the thin clouds, but there are greater maritime/continental large droplet concentration contrasts in the thin clouds that are even greater for the largest droplet sizes. Relationships among the four large cloud droplet concentrations in Fig. 6 are commensurate with corresponding L_d relationships in Table 6; i.e., there are a factor of 2 more large droplets and L_d for thick maritime compared to thick continental and for thick continental compared to thin maritime. The thin maritime clouds exceed the thin continental clouds in both large droplets and L_d by more than a factor of 2. These consistent correspondences between large cloud droplets and drizzle in the four cloud types suggest that the drizzle drops (50–620 μm diameter) may have grown by coalescence (autoconversion) of the largest cloud droplets (30–50 μm diameter).

Figure 7 shows average spectra for very thin ASTEX clouds (cd < 20 mb), which have similar N_c(av) but smaller MD than the thin clouds, especially for maritime. The continental N_c(av) of 151 cm^{-3} for these very thin clouds are comparable to the average observed continental N_{CCN}(0.02%) of 114 cm^{-3}. This is probably because the equilibrium diameter of 0.02% critical S (S_c) nuclei even at 100% relative humidity is 2 μm, which is the approximate FSSP threshold diameter. By these same arguments even if the observed 30 μm diameter droplets are also only in equilibrium at just 100% relative humidity, they could have been grown on CCN with S_c of 0.0013%. These particles have dry diameters of at least 2 μm, which is approximately the lower size limit of giant nuclei. Feingold et al. (1999) considered concentrations of 10^{-2} to 10^{-3} cm^{-3} for 10 μm diameter and larger salt particles. These would have equilibrium sizes at 100% relative humidity of at least 200 μm. This analysis suggests that Fig. 7 indicates that giant nuclei may exist at concentrations no greater than those of the largest cloud droplets, $\sim 10^{-2}$ cm^{-3}. In these long-lived stratus clouds giant nuclei would have a better chance to approach equilibrium sizes than in shorter-lived clouds such as those in the Small Cumulus Microphysics Study (SCMS) (HY01), where, by these same arguments for measured large droplets near cloud base, there also did not appear to be more giant nuclei in maritime than continental.

The 17-fold maritime/continental difference in L_d for thin ASTEX stratus is closer to the factor of 40 or 14 differences in drizzle that was predicted by Feingold et al. (1999) for approximately 50 mb thick stratus clouds with droplet concentration differences of 250 versus 150 cm^{-3} and 150 versus 50 cm^{-3}, respectively, when giant nuclei were not included. When giant nuclei were included in those calculations, Feingold et al. (1999) predicted only factor of 2 differences in drizzle. The very thin

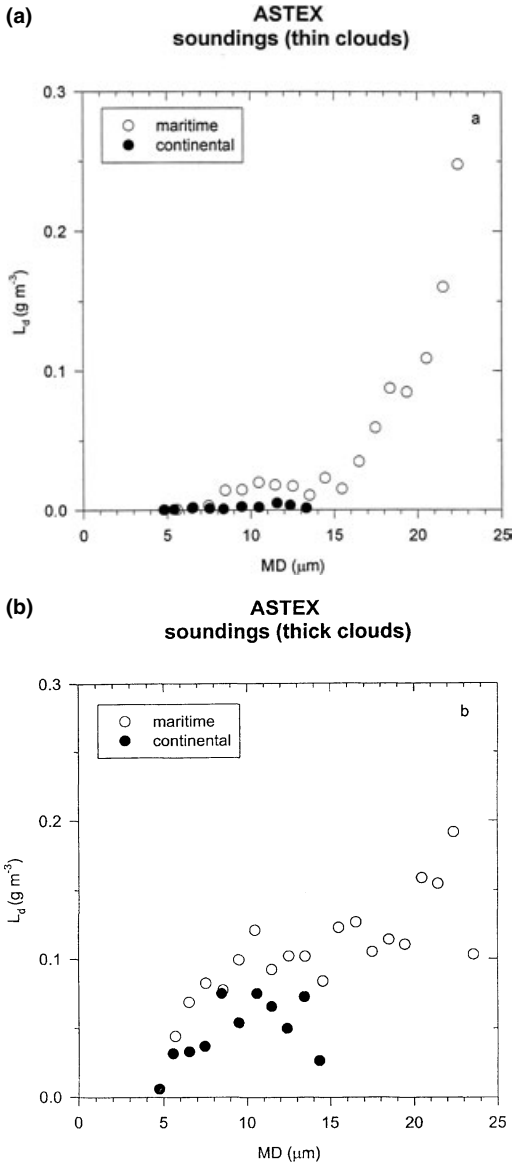

Fig. 4. Bin-averaged drizzle (50–620 μm diameter) liquid water content (L_d) versus mean diameter (MD) of cloud droplets (2–50 μm diameter) for (a) thin (cd < 45 mb) and (b) thick (cd > 45 mb) ASTEX clouds. MD bin size is 1 μm.

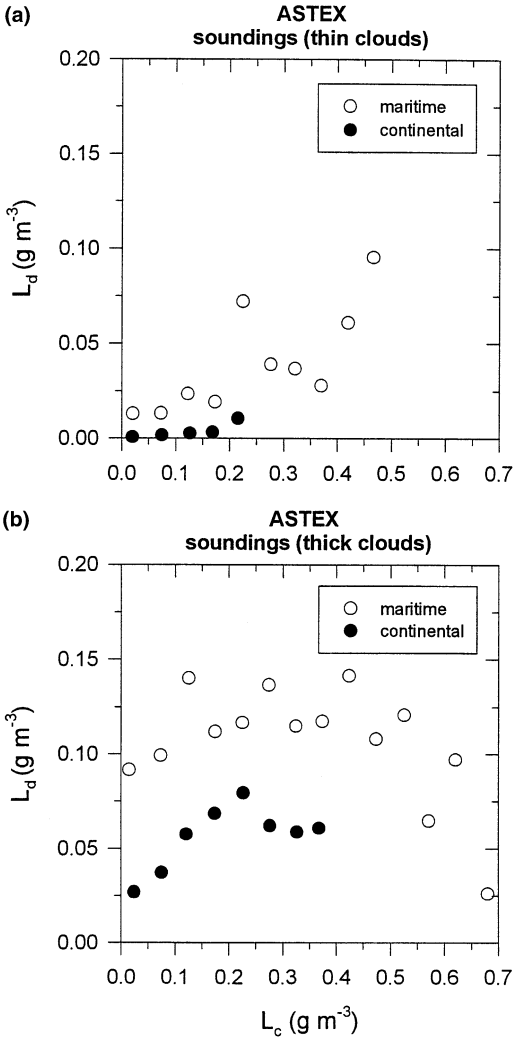

Fig. 5. Bin-averaged drizzle liquid water content (L_d) versus cloud droplet liquid water content (L_c) (for droplets 2–50 μm diameter) for (a) thin (cd < 45 mb) and (b) thick (cd > 45 mb) ASTEX clouds. L_c bin size is 0.05 g m^{-3}.

clouds of Fig. 7, which should better reflect the influences of the pre-existing aerosol (CCN) rather than the effects of cloud dynamics, i.e., droplet growth in thicker clouds, suggest no significant maritime/continental differences in giant nuclei concentrations. The longer growth times allowed in the thicker clouds then produce the higher concentrations of large and largest cloud droplets and drizzle that are observed in the maritime clouds. This difference is more likely attributable to lower total cloud droplet concentrations in maritime clouds due to lower N_{CCN} rather than to greater concentrations of giant nuclei in the maritime air. In fact Fig. 7 suggests fewer maritime

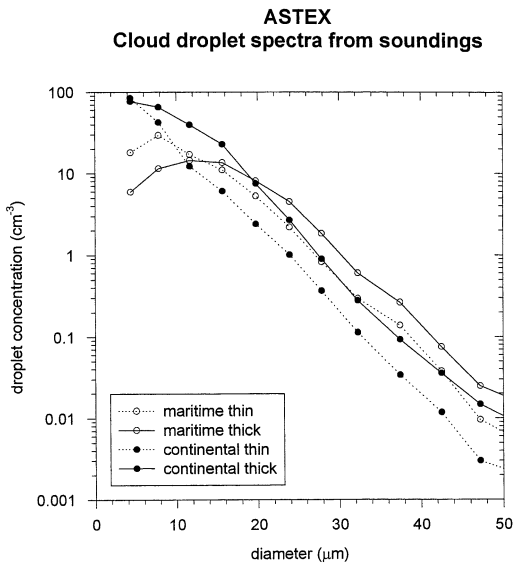

Fig. 6. As Fig. 1 for ASTEX only but with a log scale.

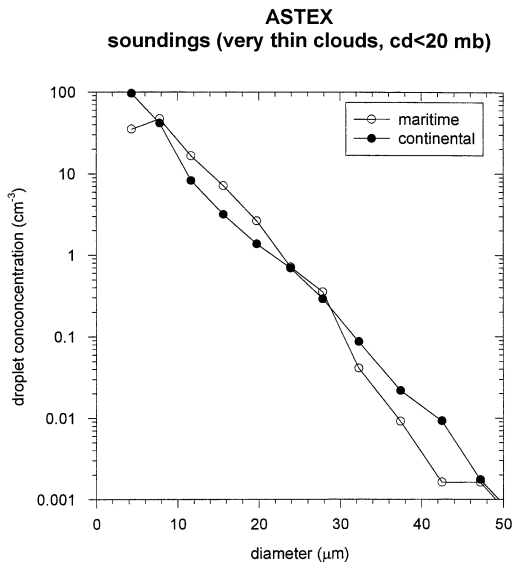

Fig. 7. As Fig. 6 but for very thin (cd < 20 mb) clouds only.

giant nuclei. This analysis for thin stratus suggests that the application of Feingold et al. (1999) to the cumulus clouds of SCMS may not have been so much of a stretch as HY01 had noted. Therefore HY01 and this analysis suggest that continental/maritime differences in giant nuclei were probably not an important factor in the observed continental/maritime precipitation differences in either SCMS or ASTEX.

4. Summary and comparisons with previous work

The correlations and ratios between flight-averaged N_{CCN} and flight-averaged and binmax cloud droplet concentrations (N_c) in Table 2 are similar to HY01. That study (SCMS) and ASTEX had the advantage of contrasting air masses to draw better correlations. Nonetheless, the maritime data of FIRE did show good N_{CCN}–N_c correlations especially for binmax, though only five data points offers limited statistical significance. The near-adiabatic cloud parcels showed similar CCN–droplet concentration correlations to those found in pristine maritime air of the Southern Ocean in the First Aerosol Characterization Experiment (ACE 1) (Yum et al., 1998).

The predictions of cloud droplet concentrations (N_p) based on CCN spectra and updrafts (FIRE only; Table 4) showed similar correlation coefficients to the best CCN–droplet concentration relationships of Tables 2 and 3. The model predictions were better because of lower regression intercepts and slopes, and ratios with measured droplet concentrations that are closer to 1.0. The model predictions (N_p) are superior mainly because they can account for the different cloud supersaturations. In spite of a smaller range of concentrations, this regression for near-adiabatic parcels was almost identical to the same regression for ACE 1 (Yum et al., 1998). When these 27 N_p–N_c(parcel) data points from FIRE and ACE 1 are combined, the correlation coefficient is 0.79, which is well above the 99.95% significance level. Moreover the intercept of this combined regression is only -2 and the slope is 1.15 with an average ratio of N_p to N_c of 1.17. These results indicate good CCN–cloud droplet closure. In Atlantic stratus Snider and Brenguier (2000) also found a rather linear relationship between droplet concentration predictions and measurements.

All three effective supersaturation (S_{eff}) estimates for these two maritime air masses straddled ACE 1 (Yum et al., 1998) and SCMS (HY01) S_{eff}; i.e., for N_c(av) S_{eff} was 0.08 and 0.31% for FIRE and ASTEX, respectively, compared to 0.15 and

0.20% for ACE 1 and SCMS, respectively; S_{eff} for N_{binmax} was 0.48 and >1.00% for FIRE and ASTEX, respectively compared to 0.89% for ACE 1 (not reported for SCMS); S_{eff} for N_c(parcel) was 0.19 and >1.00% for FIRE and ASTEX, respectively, compared to 0.48% for ACE 1 (could not be done for SCMS). The higher N_{CCN} of SCMS maritime (it was really modified maritime as N_c was twice that of ASTEX; HY01) may account for the lower S_{eff} there in spite of higher updrafts (W) of the cumuli.

The ASTEX continental S_{eff} for N_c(av) of 0.04% was lower than SCMS continental S_{eff} for N_c(av) of 0.12% (HY01). This may be due to the higher W in the cumuli of SCMS or to the noted underestimates of cloud droplet concentrations in ASTEX continental. Undercounting was less a problem in SCMS because those cumulus cloud droplets were larger (MD = 11 μm versus 8 μm; HY01). Other continental S_{eff} estimates were higher in SCMS probably because of the higher W of the cumulus clouds.

The ratio of the cubes of volume mean diameter to effective diameter ($K = D_v^3/D_e^3$; row 11, Table 1) were lower than the values reported by Martin et al. (1994) or HY01; $K = 0.80$ and 0.76, respectively, for maritime and 0.67 for continental by both. There was, however, the same tendency for lower values in more continental/polluted air masses.

The thin maritime stratus mean cloud droplet mean diameter (MD) threshold for drizzle of 15 μm is smaller than the 20 μm MD threshold for drizzle of small cumulus clouds (HY01) probably because of the longer lifetimes of the stratus clouds. Gerber (1996) also found a similar droplet size threshold for drizzle in maritime stratus.

5. Conclusions

These results uphold the first indirect aerosol effect, higher CCN concentrations causing higher cloud droplet concentrations. A reasonable degree of CCN–cloud droplet closure was again (Yum et al., 1998) found in maritime stratus clouds when other factors such as updraft, entrainment, and cloud scavenging were removed by using near-adiabatic cloud parcels and a model that accounted for the effects of updraft and the complete CCN spectrum.

As reported by Yum et al. (1998) there is now further evidence that stratus cloud supersaturations are higher than earlier estimates (e.g., Mason, 1971; Hudson, 1984). Proper application of this work to anthropogenically affected clouds will require better measurements of smaller cloud droplets because clouds with supersaturations (S) even as low as 0.08%, which is much smaller than the cloud S determined here, can have activated droplets smaller than the 2 μm diameter FSSP threshold.

The second indirect aerosol effect was also observed here and there was a sharp threshold droplet size for the onset of coalescence and drizzle. Rotstayn (1999) showed that precipitation is very sensitive to the value of the threshold droplet size for autoconversion. The difference in maritime/continental drizzle and the droplet size threshold are more obvious when the complexities of thicker clouds are removed. This result may have extensive implications because thin maritime stratus may rain out before achieving large vertical extents, whereas thin continental stratus may achieve greater thicknesses because they do not rain out (i.e., Pincus and Baker, 1994). Ackerman et al. (1993) discussed dynamical implications of such effects of CCN on precipitation and cloud lifetimes. Results here suggest great similarities in precipitation inhibition between stratus and small cumulus clouds (HY01).

6. Acknowledgments

This work was supported by National Aeronautics and Space Administration grants NAG-1-1113 and NAG-1-2183. We also express our appreciation and gratitude to the crew and staff of the Research Aviation Facility of the National Center for Atmospheric Research.

REFERENCES

Ackerman, A. S., Toon, O. B. and Hobbs, P. V. 1993. Dissipation of marine stratiform clouds and collapse of the marine boundary layer due to depletion of cloud condensation nuclei by clouds. *Science* **262**, 226–229.

Albrecht, B. A., Randall, D. A. and Nicholls, S. 1988. Observations of marine stratocumulus during FIRE. *Bull. Am. Meteor. Soc.* **69**, 618–626.

Albrecht, B. A. 1989. Aerosols, cloud microphysics and fractional cloudiness. *Science* **245**, 1227–1230.

Albrecht, B. A., Bretherton, C. S., Johnson, D., Schubert, W. H. and Frisch, A. S. 1995. The Atlantic Stratocumulus Transition Experiment — ASTEX. *Bull. Am. Meteor. Soc.* **76**, 889–904.

Baker, M. G., Corbin, R. G. and Latham, J. 1980. The influence of entrainment on the evolution of cloud droplet spectra; I. A model of inhomogeneous mixing. *Q. J. R. Meteorol. Soc.* **108**, 871–898.

Baumgardner, D. 1983. An analysis and comparison of five water droplet measuring instruments, *J. Appl. Meteorol.* **22**, 891–910.

Baumgardner, D. and Spowart, M. 1990. Evaluation of the forward scattering spectrometer probe. Part III: time response and laser inhomogeneity limitations. *J. Atmos. Oceanic Technol.* **7**, 666–672.

Charlson, R. J., Schwartz, S. E., Hales, J. M., Cess, R. D., Coakley, Jr., J. A., Hansen, J. E. and Hofmann, D. J. 1992. Climate forcing by anthropogenic aerosols. *Science* **255**, 423–430.

Feingold, G., Cotton, W. R., Kreidenweis, S. M. and Davis, J. T. 1999. The impact of giant cloud condensation nuclei on drizzle formation in stratocumulus: implications for cloud radiative properties. *J. Atmos. Sci.* **56**, 4100–4117.

Gerber, H. 1996. Microphysics of marine stratocumulus clouds with two drizzle modes. *J. Atmos. Sci.* **53**, 1649–1662.

Hudson, J. G. 1984. CCN measurements within clouds. *J. Climat. Appl. Meteorol.* **23**, 42–51.

Hudson, J. G. 1993. Cloud condensation nuclei. *J. Appl. Meteorol.* **32**, 596–607.

Hudson, J. G. and Li, H. 1995. Microphysical contrasts in Atlantic stratus. *J. Atmos. Sci.* **52**, 3031–3040.

Hudson, J. G. and Xie, Y. 1999. Vertical distributions of cloud condensation nuclei spectra over the summertime northeast Pacific and Atlantic Oceans. *J. Geophys. Res.* **104**, 30,219–30,229.

Hudson, J. G. and Yum, S. S. 1997. Droplet spectral broadening in marine stratus. *J. Atmos. Sci.* **54**, 2642–2654.

Hudson, J. G. and Yum, S. S. 2001. Maritime-continental drizzle contrasts in small cumuli. *J. Atmos. Sci.* **58**, 915–926.

Knollenberg, R. G. 1981. Techniques for probing cloud microstructure. In: *Clouds: their formation, optical properties and effects* (eds. P. V. Hobbs and A. Deepak) Academic Press, 494 pp.

Martin, G. M., Johnson, D. W. and Spice, A. 1994. The measurement and parameterization of effective radius of droplets in warm stratocumulus clouds. *J. Atmos. Sci.* **51**, 1823–1842.

Mason, B. J. 1971. *The physics of clouds.* Oxford University Press, 671 pp.

Nicholls, S. 1984. The dynamics of stratocumulus: aircraft observations and comparisons with a mixed layer model. *Q. J. R. Meteorol. Soc.* **110**, 783–820.

Pincus, R. and Baker, M. B. 1994. Effects of precipitation on the albedo susceptibility of clouds in the marine boundary layer. *Nature* **372**, 250–252.

Robinson, N. F. 1984. The efficient numerical calculation of condensational cloud drop growth. *J. Atmos. Sci.* **41**, 697–700.

Rosenfeld, D. 1999. TRMM observed first direct evidence of smoke from forest fires inhibiting rainfall. *Geophys. Res. Lett.* **26**, 3105–3108.

Rosenfeld, D. 2000. Suppression of rain and snow by urban and industrial air pollution. *Science* **287**, 1793–1796.

Rotstayn, L. D. 1999. Indirect forcing by anthropogenic aerosols: a global climate model calculation of the effective-radius and cloud-lifetime effects. *J. Geophys. Res.* **104**, 9369–9380.

Snider, J. R. and Brenguier, J. L. 2000. Cloud condensation nuclei and cloud droplet measurements during ACE-2. *Tellus* **52B**, 828–842.

Twohy, C. H. and Hudson, J. G. 1995. Cloud condensation nuclei spectra within maritime cumulus cloud droplets. *J. Appl. Meteorol.* **34**, 815–833.

Twomey, S. 1959. The supersaturation in natural clouds and the variation of cloud droplet concentration. *Geofis. Pura Appl.* **43**, 243–249.

Twomey, S. 1977. The influence of pollution on the shortwave albedo of clouds. *J. Atmos. Sci.* **34**, 1149–1152.

Twomey, S. and Warner, J. 1967. Comparison of measurements of cloud droplets and cloud nuclei. *J. Atmos. Sci.* **24**, 702–703.

Warner, J. 1973. The microstructure of cumulus cloud. Part IV. The effect on the droplet spectrum of mixing between cloud and environment. *J. Atmos. Sci.* **30**, 256–261.

Yum, S. S., Hudson, J. G. and Xie, Y. 1998. Comparisons of cloud microphysics with cloud condensation nuclei spectra over the summertime Southern Ocean. *J. Geophys. Res.* **103**, 16,625–16,636.